


Estimating soil erosion and sediment yield using geographic information systems in southeastern Morocco: The case of the high and middle Drâa watershed

Zahli Saleh Eddine^{1*} 

¹ Department of Geography, Faculty of Letters and Human Sciences, University of Hassan II, Ain Chock, Casablanca, Morocco

E-mail: salahzahli16@gmail.com

ABSTRACT

Soil erosion and sediment transfer represent major environmental challenges in semi-arid regions of southern Morocco, particularly in large watersheds characterized by strong topographic contrasts and fragile environmental conditions. This study assesses soil loss, sediment delivery, and channel sediment yield in the High and Middle Drâa watershed using a GIS-based implementation of the revised universal soil loss equation (RUSLE) combined with sediment delivery ratio (SDR) analysis. Climatic data, land use and land cover information, soil properties, and a 30 m resolution digital elevation model were processed within the ArcGIS environment to derive the spatial distribution of erosion-related factors and quantify sediment dynamics. The results reveal a marked spatial heterogeneity of soil erosion intensity across the watershed. Very slight and slight erosion classes dominate in terms of area, covering about 61.7% of the basin, but contribute less than 4% of the total soil loss. In contrast, very high and extreme erosion classes together account for approximately 22.2% of the watershed area while generating more than 81% of the total annual soil loss. The estimated total soil loss reaches about 6 366 005 tons per year, with an average soil loss rate of approximately 46.2 t ha⁻¹ yr⁻¹. Sediment delivery analysis indicates an average SDR value of about 0.17, highlighting a limited efficiency of sediment transfer from hillslopes to the drainage network. Channel sediment yield ranges from less than 5 to more than 20 t ha⁻¹ yr⁻¹, with severe sediment yield classes representing only 21.7% of the channel surface but contributing over 70% of the total sediment delivered, estimated at approximately 1.09 million tons per year. The scientific contribution of this study is the quantitative identification of a spatial and functional decoupling between soil erosion intensity and sediment export, with sediment dynamics primarily controlled by slope, drainage connectivity, and land cover.

Keywords: soil erosion, sediment yield, sediment delivery ratio, High and Middle Drâa watershed, southern Morocco.

INTRODUCTION

Soil erosion by water is widely recognized as one of the most serious forms of land degradation in semi-arid and arid regions, where fragile environmental conditions, irregular rainfall regimes, and limited vegetation cover combine to intensify surface runoff and sediment detachment (Wischmeier and Smith, 1978; Renard et al., 1997). The progressive removal of fertile topsoil not only reduces agricultural productivity but also accelerates downstream sedimentation, channel

instability, and reservoir siltation, thereby threatening water resources and ecosystem sustainability (Morgan, 2005; Belasri and Lakhouili, 2016). These impacts are particularly pronounced in Mediterranean and North African environments, where climatic variability, episodic high-intensity rainfall events, and increasing human pressure have amplified erosion processes over recent decades, as demonstrated by several GIS-based erosion assessments conducted in Moroccan and Mediterranean watersheds (Sadiki et al., 2004; Bou-Imajjane et al. 2020).

In Morocco, soil erosion constitutes a major environmental challenge, particularly in large watersheds characterized by strong topographic contrasts, highly erodible lithologies, and heterogeneous land-use patterns (Sadiki et al., 2004; Belasri and Lakhouili, 2016). Numerous studies have demonstrated that erosion rates vary considerably across Moroccan basins as a function of rainfall erosivity, soil physical properties, slope morphology, vegetation cover, and land management practices (Bou-Imajjane et al. 2020; El Jazouli et al., 2017). Consequently, spatially explicit approaches based on GIS and erosion modeling have become essential tools to accurately capture the spatial variability of erosion processes and to identify critical sediment source areas that require priority conservation and land-management interventions (Renard et al., 1997; Meliho et al., 2023).

Geographic information systems (GIS), combined with empirical soil erosion models, have become a standard and effective framework for assessing soil erosion at the watershed scale, as they allow the integration of topographic, climatic, pedological, and land-use data within a spatially explicit analytical environment (Renard et al., 1997; Sadiki et al., 2004). Among these models, the revised universal soil loss equation (RUSLE) has been extensively applied in Mediterranean and semi-arid regions due to its conceptual robustness, adaptability to GIS environments, and relatively moderate data requirements compared to physically based models (Wischmeier and Smith, 1978; Belasri and Lakhouili, 2016). RUSLE estimates average annual soil loss by integrating rainfall erosivity (R), soil erodibility (K), topographic factors related to slope length and steepness (LS), land cover and management (C), and conservation practices (P), thereby enabling detailed mapping of erosion susceptibility and spatial variability of erosion risk across heterogeneous landscapes (Moore and Burch, 1986; El Jazouli et al., 2017).

The GIS-based implementation of RUSLE enables the integration of multi-source spatial datasets, including digital elevation models, climatic records, soil maps, and land-use information, to generate high-resolution erosion maps and spatially explicit assessments of soil loss (Renard et al., 1997; Sadiki et al., 2004). Such maps provide valuable insights into the spatial variability of erosion processes and facilitate the identification of areas most exposed to soil degradation (Moore

and Burch, 1986). Previous applications of GIS-based RUSLE in northern and central Morocco have demonstrated its effectiveness in quantifying erosion risk and supporting soil conservation planning at both local and regional scales (El Jazouli et al., 2017; Belasri and Lakhouili, 2016).

The High and Middle Drâa watershed, located in southern Morocco, constitutes one of the most environmentally sensitive hydrological systems in the region. Extending from the southern slopes of the High Atlas Mountains toward the central Drâa Valley, the basin includes steep mountainous headwaters, intermediate plateaus, and wide alluvial corridors. This area is characterized by low and highly variable rainfall, episodic high-intensity storm events, sparse and discontinuous vegetation cover, and increasing land-use pressure related to irrigated agriculture, grazing, and infrastructure development (Johannsen et al., 2016; Mattingly et al., 2018). These combined geomorphological, climatic, and anthropogenic factors make the High and Middle Drâa basin particularly vulnerable to water-induced soil erosion and sediment transfer processes (Boudhar et al., 2009; Amellah and el Morabiti, 2021).

Despite its strategic importance for water resources and regional development, comprehensive spatial assessments of soil erosion in the High and Middle Drâa basin remain limited. Existing studies in this region have primarily focused on hydrological variability, groundwater resources, and climate change impacts, while basin-scale evaluations explicitly addressing soil erosion patterns and their controlling factors are still scarce (Johannsen et al., 2016; Mattingly et al., 2018). This lack of spatially explicit erosion assessments constrains the development of effective soil conservation strategies and sustainable land management policies adapted to the environmental constraints of the Drâa basin (Boudhar et al., 2009).

Despite the extensive application of GIS-based RUSLE modeling in semi-arid regions, most studies remain limited to mapping soil loss patterns and rarely examine how erosion intensity translates into effective sediment export at the scale of large watersheds (Johannsen et al., 2016; Mattingly et al., 2018). In particular, the functional relationship between hillslope erosion, internal sediment storage, and drainage connectivity remains insufficiently explored in large, topographically heterogeneous basins such as the High and Middle Drâa watershed (Boudhar et al., 2009).

This study addresses this gap by focusing on the High and Middle Drâa watershed as an integrated geomorphic system rather than a simple erosion-prone area. The central hypothesis is that, in large semi-arid watersheds, zones of maximum soil erosion do not necessarily control sediment export due to strong spatial variability in connectivity and internal sediment trapping. Accordingly, the study aims to (1) quantitatively distinguish erosion-dominated areas from sediment-export-controlling zones, (2) identify the geomorphological and land-cover factors governing this decoupling, and (3) assess how slope, drainage connectivity, and land use jointly regulate sediment dynamics at the basin scale.

By explicitly linking erosion intensity to sediment transfer efficiency, this study seeks to generate process-based insight into the functional behavior of sediment dynamics in the High and Middle Drâa watershed and to support targeted soil and water conservation planning in large semi-arid environments (Sadiki et al., 2004; Belasri and Lakhouili, 2016).

METHODS AND MATERIALS

Study area

The study area corresponds to the High and Middle Drâa watershed, located in southern Morocco, (Figure 1). The basin extends from the

southern slopes of the High Atlas Mountains toward the pre-Saharan domains and covers a wide altitudinal range, with elevations varying approximately from 450 m in the downstream plains to over 4000 m in the mountainous headwaters. This pronounced topographic gradient controls drainage organization, slope morphology, and hydrological responses across the basin (Johannsen et al., 2016).

The High and Middle Drâa basin is characterized by a semi-arid to arid climate, marked by low and irregular annual rainfall, strong interannual variability, and episodic high-intensity storm events. These climatic conditions, combined with steep slopes in the upstream areas and sparse vegetation cover, favor intense surface runoff and enhance susceptibility to water-induced soil erosion (Sadiki et al., 2004; Boudhar et al., 2009). The drainage network exhibits a dendritic pattern controlled by structural and lithological contrasts, with ephemeral channels dominating most of the basin.

Methodologies and data sets

In the context of this study, soil erosion in the High and Middle Drâa basin was evaluated using a GIS-based implementation of the RUSLE. The RUSLE model estimates the average annual soil loss (A , $t \cdot ha^{-1} \cdot yr^{-1}$) as the product of five erosion-controlling factors according to the equation:

$$A = R \times K \times LS \times C \times P \quad (1)$$

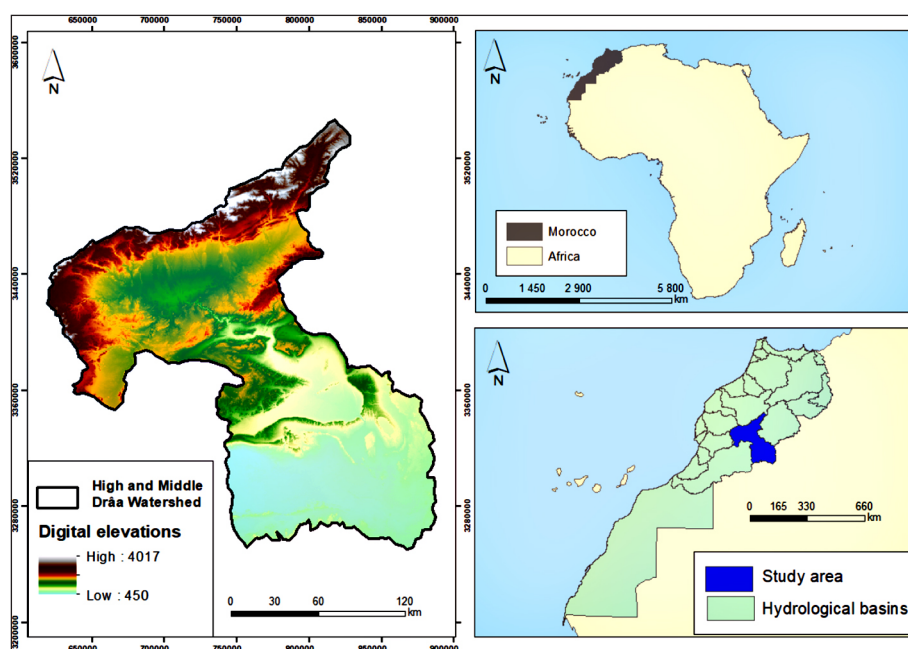


Figure 1. The High and Middle Drâa watershed

where: R represents the rainfall erosivity factor ($\text{MJ}\cdot\text{mm}\cdot\text{ha}^{-1}\cdot\text{h}^{-1}\cdot\text{yr}^{-1}$), K denotes the soil erodibility factor ($\text{t}\cdot\text{h}\cdot\text{h}\cdot\text{ha}^{-1}\cdot\text{MJ}^{-1}\cdot\text{mm}^{-1}$), LS corresponds to the topographic factor combining slope length and steepness, C represents the land cover and management factor, and P refers to the conservation practice factor (Wischmeier & Smith, 1978; Renard et al., 1997).

The estimation of these parameters was based on multi-source spatial datasets derived from climatic records, soil databases, topographic data, and satellite imagery. Rainfall, soil, topography, and land-use data used for the computation of RUSLE factors, along with their spatial resolution and sources, are summarized in Table 1. All datasets were processed and harmonized at a spatial resolution of 30 m within a Geographic Information System environment to ensure consistent spatial analysis across the study area.

Although recent machine-learning approaches have shown promising performance in soil erosion prediction, their application generally requires large, spatially consistent training datasets and long-term ground observations, which remain limited in large semi-arid watersheds such as the High and Middle Drâa. In this context, the use of RUSLE is justified by its transparent structure, explicit representation of controlling factors, and suitability for data-scarce environments. More importantly, the objective of this study is not solely predictive accuracy, but the analysis of

functional relationships between erosion intensity, sediment delivery, and landscape connectivity. RUSLE allows direct interpretation of the individual roles of slope, land cover, rainfall erosivity, and conservation practices, thereby providing a conceptually appropriate framework for addressing the research questions of this study.

All primary datasets used in this study originate from widely recognized and quality-controlled sources, including satellite-based products and international soil databases, ensuring reliable and consistent spatial erosion analysis in the High and Middle Drâa watershed.

RUSLE configuration and GIS implementation

RUSLE was implemented using a fully raster-based GIS workflow at a spatial resolution of 30 m. All factor layers (R, K, LS, C, and P) were generated or resampled to a common grid and harmonized to the same coordinate system (UTM Zone 29N), cell size, and spatial extent corresponding to the High and Middle Drâa watershed boundary.

Soil loss (A) was calculated for each raster cell by multiplying the spatially distributed RUSLE factors using the Raster Calculator according to the equation $A = R \times K \times LS \times C \times P$, following the methodological framework illustrated in Figure 2. To ensure spatial consistency and reproducibility, GIS processing environments were fixed as follows: cell size = 30 m, snap raster = 30 m DEM, and analysis extent and mask limited to the watershed boundary. Zonal statistics were subsequently applied to derive mean

Table 1. Study data and data sources used for soil erosion assessment in the High and Middle Drâa basin

Data	Description	Spatial resolution	Source
Rainfall	Long-term mean annual rainfall data derived from meteorological stations and regional climatic records	Interpolated to 30 m	National meteorological services and regional hydrological agencies; complementary global datasets
Soil	Soil physical properties (% sand, % silt, % clay) used to derive soil erodibility (K factor)	30 m	FAO Digital Soil Map of the World (DSMW) and Harmonized World Soil Database
Topography	Digital Elevation Model used to extract slope, flow direction, flow accumulation, and LS factor	30 m	SRTM DEM (USGS Earth Explorer)
Land use / Land cover	Land use and land cover classes used to derive cover-management factor (C)	30 m	Landsat 8 OLI imagery (USGS / NASA Earth Explorer)
Conservation practices	Support practice information used to estimate P factor based on slope classes and land management assumptions	30 m	Derived from land use, slope map, and literature-based coefficients
Drainage network	Stream network extracted from DEM and used for erosion–sediment connectivity analysis	30 m	DEM-based hydrological analysis (ArcGIS 10.1)
Soil erosion	Estimated average annual soil loss using the RUSLE model	30 m	Computed in GIS environment

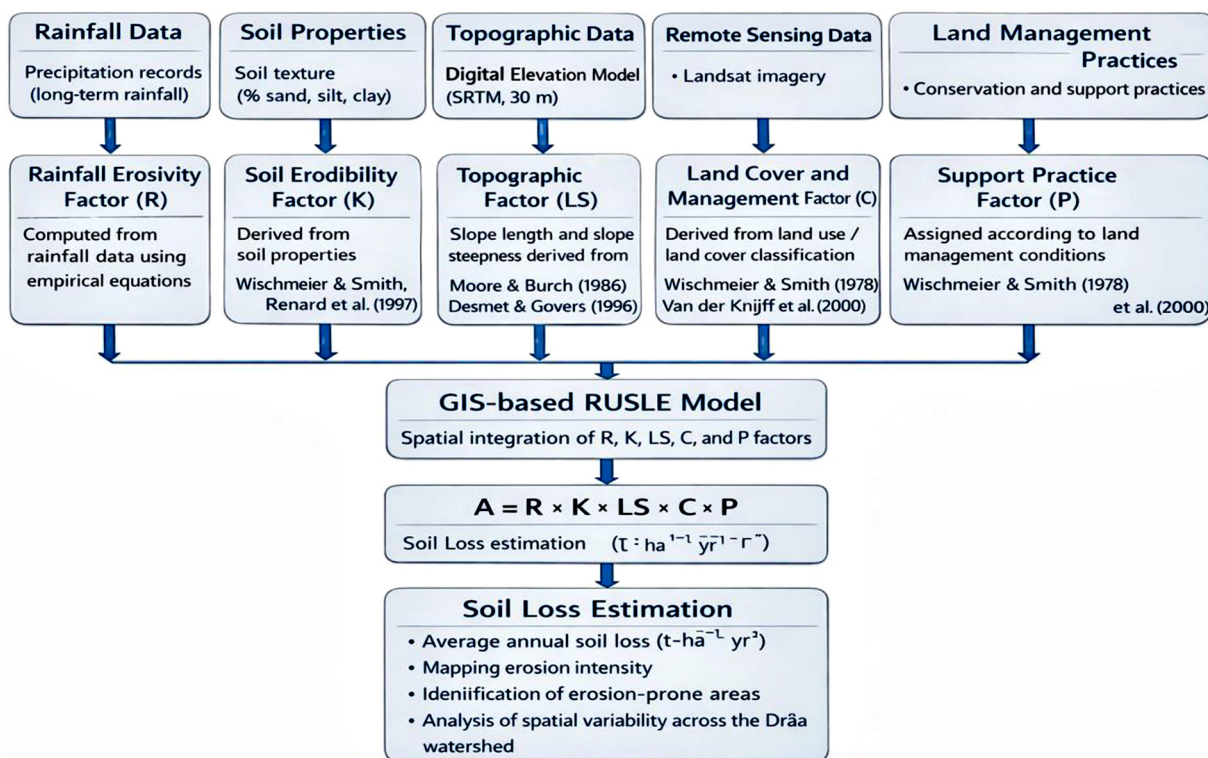


Figure 2. Schematic illustration of methods

soil loss rates and class-based contributions at the watershed scale.

All spatial analyses and RUSLE computations were performed using ArcGIS Desktop 10.1 with the Spatial Analyst extension, while drainage attributes required for sediment delivery analysis were derived using ArcHydro tools. As an empirical deterministic and non-iterative model, RUSLE does not involve model training or iterative calibration. Methodological robustness was ensured through sensitivity checks on key GIS-derived parameters, particularly those related to drainage delineation for channel slope and SDR estimation. The stability of spatial patterns across parameter values indicates that the results are not sensitive to a specific parameter choice.

The mean annual soil loss rate ($t \cdot ha^{-1} \cdot yr^{-1}$) was calculated as the spatial average of the RUSLE-derived soil loss raster across the entire watershed using zonal statistics within the GIS environment. This spatially averaged value represents a cell-based mean erosion rate rather than a simple division of total soil loss by the basin area

Rainfall erosivity factor

The rainfall erosivity factor (R) was estimated to characterize the spatial variability of rainfall aggressiveness over the High and Middle Drâa

watershed (Figure 3b). Due to the lack of high-resolution rainfall intensity data, R was calculated using long-term precipitation records based on the empirical formulation proposed by Rango and Arnoldus, which has been widely applied in semi-arid and Mediterranean environments (Wischmeier and Smith, 1978; Zema et al., 2018).

Mean monthly precipitation data were compiled for the period 2000–2024 and used to derive annual rainfall totals for each meteorological station. Rainfall erosivity was then computed using the equation:

$$R = 10^{(1.74 \log_{10} [\sum (P_i^2 / P)] + 1.29)} \quad (2)$$

where: P_i represents the mean precipitation of month i (mm), and P denotes the mean annual precipitation (mm). This formulation accounts for the seasonal concentration of rainfall, which is a key driver of erosion processes in semi-arid regions characterized by irregular and episodic precipitation patterns (Zema et al., 2018).

The calculated R values, expressed in $MJ \cdot m \cdot ha^{-1} \cdot h^{-1} \cdot yr^{-1}$, were spatially interpolated using the inverse distance weighting (IDW) method at a 30-m resolution within a GIS environment. As shown in Figure 3b, rainfall erosivity exhibits a marked spatial gradient, with higher values in the

northern mountainous sectors influenced by orographic effects, and progressively lower values toward the southern arid areas of the basin. This spatial pattern reflects the combined influence of altitude, climatic variability, and rainfall distribution across the Drâa watershed, consistent with observations reported for other Moroccan semi-arid basins (Wischmeier and Smith, 1978; Zema et al., 2018).

Soil erodability factor

The soil erodibility factor (K) was estimated to represent the intrinsic susceptibility of soils to detachment and transport by rainfall and surface runoff. In this study, K was derived from soil unit information obtained from the FAO digital soil map of the world (DSMW) and the Harmonized World Soil Database. Although the EPIC/Williams (1996) formulation expresses soil erodibility as a product of texture- and organic-matter-related sub-factors (fcsand, fclsi, forgC, and fhisand), the detailed and spatially continuous soil property measurements required to compute these sub-factors were not consistently available at the scale of the High and Middle Drâa watershed. Consequently, representative K values were

assigned to the dominant FAO soil units based on ranges reported in the literature for semi-arid environments (Wischmeier and Smith, 1978; Panagos et al., 2015). These values were subsequently spatially mapped within the GIS environment to produce the K-factor raster at 30 m resolution. The soil data sources and parameters used for K factor estimation are summarized in Table 1, while the spatial distribution of soil erodibility across the watershed is illustrated in Figure 3d.

Topographic factor

The topographic factor (LS) expresses the influence of terrain morphology on water-induced soil erosion by integrating both slope length (L) and slope steepness (S) at the grid-cell scale. Slope length represents the distance over which surface runoff accumulates before sediment deposition occurs or before runoff enters a defined channel, while slope steepness controls the erosive power of flowing water. In this study, the LS factor was derived from a 30 m resolution digital elevation model by calculating slope gradient and flow accumulation within a GIS environment. The computation followed the widely adopted formulation proposed by Mitasova et al. (1996),

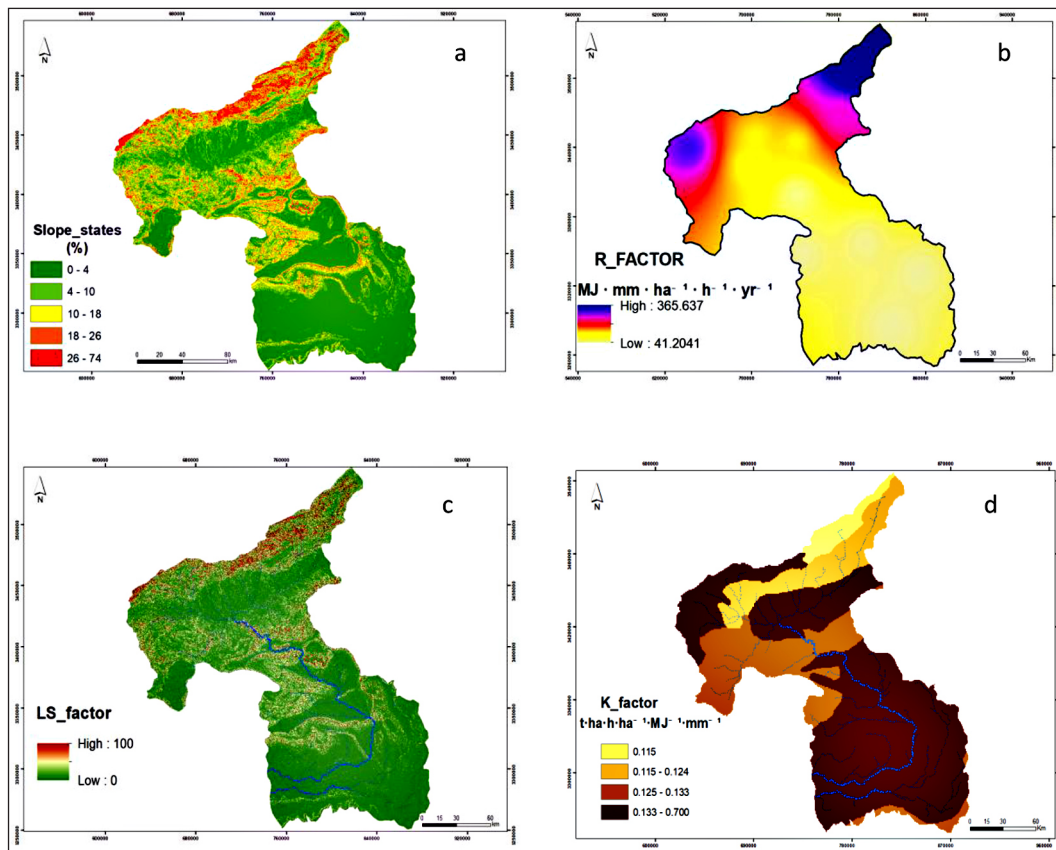


Figure 3. Slope class (a), R factor (b), LS factor (c), and K factor (d) of the High and Middle Drâa watershed

which is commonly used in RUSLE-based erosion assessments:

$$LS = (Flow\ accumulation \times Cell\ size / 22.13)^{0.4} \times (sin\ slope / 0.0896)^{1.3} \quad (3)$$

The resulting LS factor map (Figure 3c) reveals pronounced spatial variability across the High and Middle Drâa watershed. High LS values are concentrated in the upstream mountainous sectors of the High Atlas, where steep slopes and dense drainage networks prevail, indicating a strong topographic control on erosion processes. In contrast, low LS values dominate the central and downstream areas characterized by gentler slopes and broader valley floors. This spatial pattern highlights the critical role of relief in controlling erosion susceptibility in the Drâa basin and is consistent with findings reported for other semi-arid Moroccan watersheds (Sadiki et al., 2004; Khalil Issa et al., 2014).

Cover factor

The cover management factor (C) reflects the protective effect of vegetation cover and land-use conditions against soil erosion by water. High C values indicate sparse to nearly absent vegetation cover, resulting in greater soil exposure to rainfall and runoff, whereas low C values correspond to areas where vegetation, although generally limited, provides a certain degree of surface protection (Wischmeier and Smith, 1978).

In the present study, the C factor was derived from a Landsat-8 image acquired on 03/05/2023 through the calculation of the normalized difference vegetation index (NDVI) and its transformation into C values using the empirical relationship proposed by De Jong (1994):

$$C = 0.431 - 0.805 \times NDVI \quad (4)$$

Resulting values were constrained to the range [0–1] to ensure consistency with the RUSLE framework.

This approach is well adapted to semi-arid environments such as the Drâa basin, where vegetation cover is discontinuous and strongly controlled by water availability.

As illustrated in Figure 4b, high C values dominate most of the High and Middle Drâa watershed, indicating extensive areas characterized by very sparse or absent vegetation cover. These zones correspond mainly to plateaus, slopes, and arid sectors, and are therefore highly susceptible to soil erosion. In contrast, lower C values are concentrated along the main channel of the Drâa River, as well as in parts of the western sector and locally in the northeastern area of the basin. These areas coincide with the presence of riparian vegetation and irrigated or semi-natural agricultural zones, where vegetation cover, although limited, contributes to reduced erosion intensity. This spatial pattern highlights the strong influence of hydrological conditions and land-use practices on vegetation distribution and erosion control within the Drâa watershed.

Support practice factor

The support practice factor (P) represents the effect of soil conservation and land management practices on reducing soil erosion by modifying surface runoff pathways and slope conditions relative to conventional up-and-down slope cultivation (Wischmeier and Smith, 1978). This factor accounts for practices that reduce the erosive power of rainfall and overland flow through slope adjustment, land use organization, and surface management.

In the High and Middle Drâa watershed, detailed spatial information on conservation

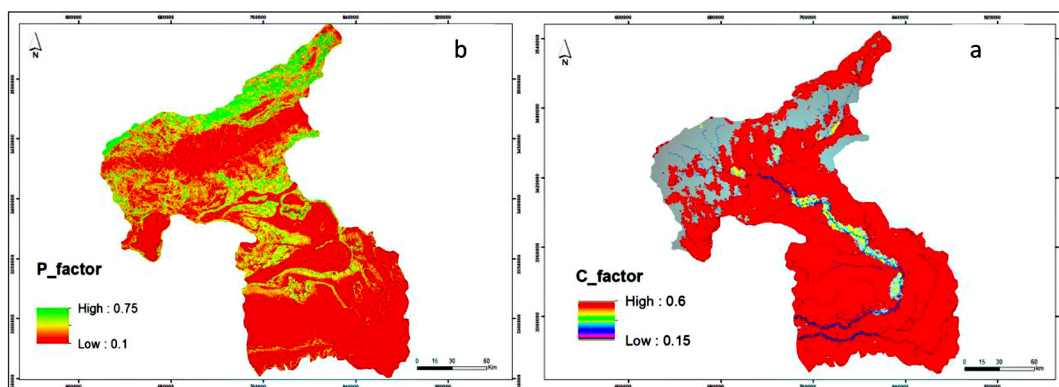


Figure 4. P factor (a) and C factor (b) of the High and Middle Drâa watershed

practices is limited. Consequently, the P factor was derived indirectly by combining land-use categories with slope classes, a commonly adopted approach in semi-arid environments characterized by heterogeneous terrain and land management conditions (Bewket and Teferi, 2009). The watershed was first classified into major land-use types, including agricultural lands, rangelands, forests, bare lands, and water bodies, and subsequently subdivided according to slope classes derived from the slope map (Table 2; Figure 4a). Each land-use–slope combination was then assigned a representative P value following the empirical formulation proposed by Werner et al., (2006):

$$P = 0.2 + 0.03 \times S \tag{5}$$

where: *S* denotes slope gradient (%).

The resulting P factor values range from 0.10 to 0.75 across the watershed (Figure 4a). Low P values dominate gently sloping agricultural areas and valley bottoms, indicating relatively effective erosion mitigation, whereas higher values are mainly associated with steep slopes and poorly managed or bare surfaces, reflecting limited conservation effectiveness and increased susceptibility to soil erosion. This spatial pattern highlights the strong control exerted by slope and land management on erosion processes within the Drâa basin.

Sediment delivery ration

The sediment delivery ratio (SDR) expresses the proportion of eroded soil that is effectively transported from hillslopes to the drainage network and ultimately exported at the watershed outlet. Not all material detached by rainfall and runoff reaches the river system, as a significant fraction is deposited along hillslopes, footslopes, and valley bottoms (Maidment, 1993; Andualem et al., 2023). SDR therefore provides a key link between potential soil erosion and actual sediment yield,

allowing a more realistic assessment of sediment transfer processes at the watershed scale.

In the present study, SDR was estimated using an empirical approach based on channel slope, which has proven particularly suitable for data-scarce semi-arid environments where sediment measurements are limited (Gebrehivot et al., 2014). The method assumes that steeper channel gradients enhance sediment transport efficiency, whereas gentler slopes favor deposition. Accordingly, SDR was calculated as a function of the average slope of drainage channels derived from the digital elevation model using ArcHydro tools, following Equation :

$$SDR = 0.627 \times SLP^{0.403} \tag{6}$$

Sediment yield (SY) at the channel scale was subsequently estimated by combining the spatially distributed soil loss derived from the RUSLE model with the sediment delivery ratio. For each raster cell, sediment yield was calculated as:

$$SY = A \times SDR \tag{7}$$

where: *SY* represents sediment yield (t·ha⁻¹·yr⁻¹), *A* is the average annual soil loss obtained from the RUSLE model (t·ha⁻¹·yr⁻¹), and *SDR* is the sediment delivery ratio. This raster-based multiplication allows the conversion of potential soil erosion into effective sediment delivery to the drainage network.

The resulting channel slope map (Figure 5) reveals spatial variability in drainage gradients across the High and Middle Drâa watershed. Higher channel slopes are mainly concentrated in upstream and structurally constrained sections of the drainage network, indicating greater sediment transfer efficiency, whereas lower gradients dominate downstream reaches and wider valley floors, where sediment deposition is more likely. These spatial patterns highlight the strong control exerted by channel morphology and topography

Table 2. Slope class distribution in the High and Middle Drâa watershed

Slope class (%)	Designation	Area (ha)	Area (%)
0–4	Flat	395 819	10.42
4–10	Gently sloping	1 570 461	41.33
10–18	Sloping	1 001 229	26.35
18–26	Strongly sloping	590 181	15.53
26–74	Steep	242 310	6.37
Total	—	3 800 000	100.00

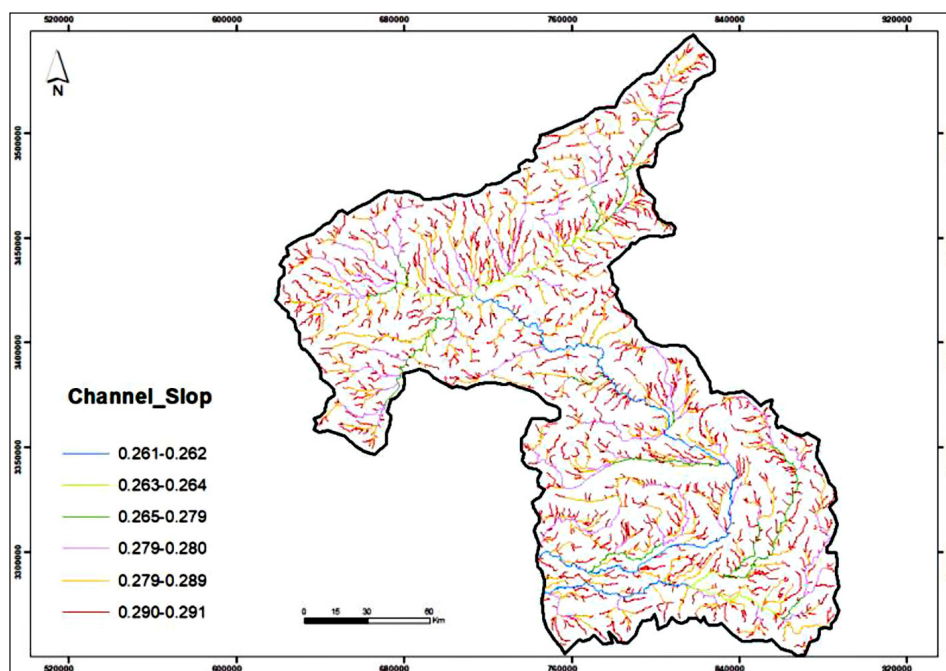


Figure 5. Channel slope map of the High and Middle Drâa watershed

on sediment connectivity and delivery processes within the Drâa basin, consistent with observations reported for other semi-arid watersheds (Gebrehivot et al., 2014).

RESULTS

Soil loss

Based on Table 3, the soil loss map (Figure 6), and the ArcGIS 10.1 processing workflow (Figure 7), the RUSLE results reveal a marked spatial heterogeneity of soil erosion intensity across the High and Middle Drâa watershed. Overall, very low to low soil loss classes ($0\text{--}14$ and $14\text{--}57\text{ t}\cdot\text{ha}^{-1}\cdot\text{yr}^{-1}$) dominate most of the watershed area, reflecting the prevalence of relatively gentle

slopes, extensive internal accumulation zones, and the mitigating role of land cover, which locally reduces the C factor.

In contrast, Figure 6 highlights spatially limited but highly erosive hotspots, mainly located in the upstream and mountainous sectors of the basin. In these areas, steep slopes (high LS factor) combine with relatively higher rainfall erosivity (R factor) and locally erodible soils (K factor), leading to moderate to extreme soil loss classes ($57\text{--}144$, $144\text{--}284$, $284\text{--}568$, and $568\text{--}916\text{ t}\cdot\text{ha}^{-1}\cdot\text{yr}^{-1}$). Although these classes occupy a small proportion of the total watershed area, they contribute disproportionately to the overall annual soil loss, a characteristic pattern of semi-arid basins where erosion is controlled by a limited number of highly connected source areas.

Table 3. Spatial distribution of soil erosion risk classes and approximate soil loss in the High and Middle Drâa watershed (Morocco)

Soil loss ($\text{t}\cdot\text{ha}^{-1}\cdot\text{yr}^{-1}$)	Erosion risk class	Area (ha)	Area (%)	Soil loss ($\text{t}\cdot\text{yr}^{-1}$)	Soil loss (%)
0–14	Very slight erosion	1 792 430	47.17	179 201	2.81
14–57	Slight erosion	553 618	14.57	51 430	0.81
57–144	Moderate erosion	391 275	10.30	368 101	5.78
144–284	High erosion	218 964	5.76	579 601	9.10
284–568	Very high erosion	421 845	11.10	2 198 502	34.54
568–916	Extreme erosion	421 868	11.10	2 990 170	46.96
Total	—	3 800 000	100.00	6 366 005	100.00

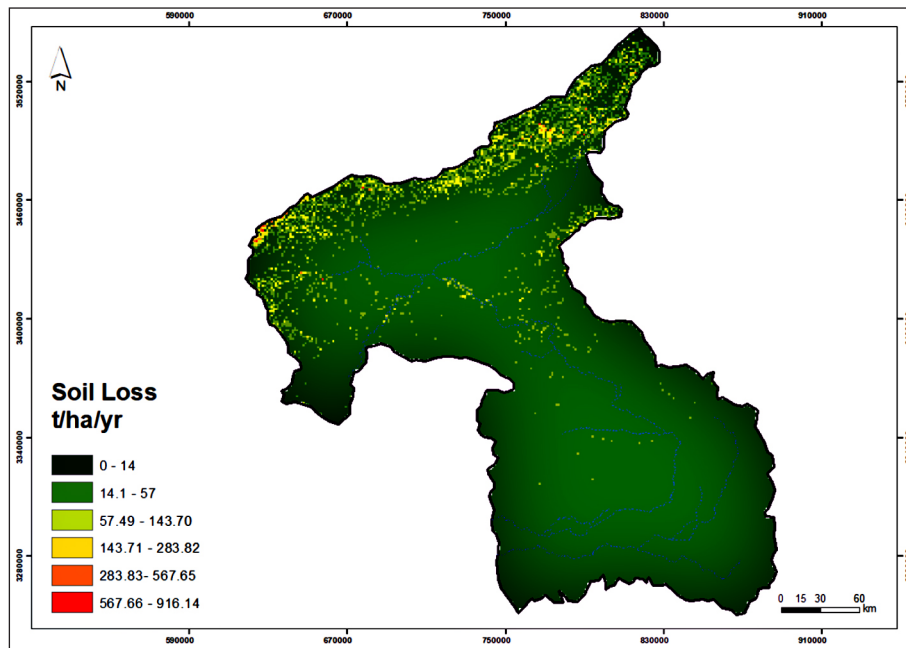


Figure 6. Soil loss of the the High and Middle Drâa watershed (Wischmeier classification)

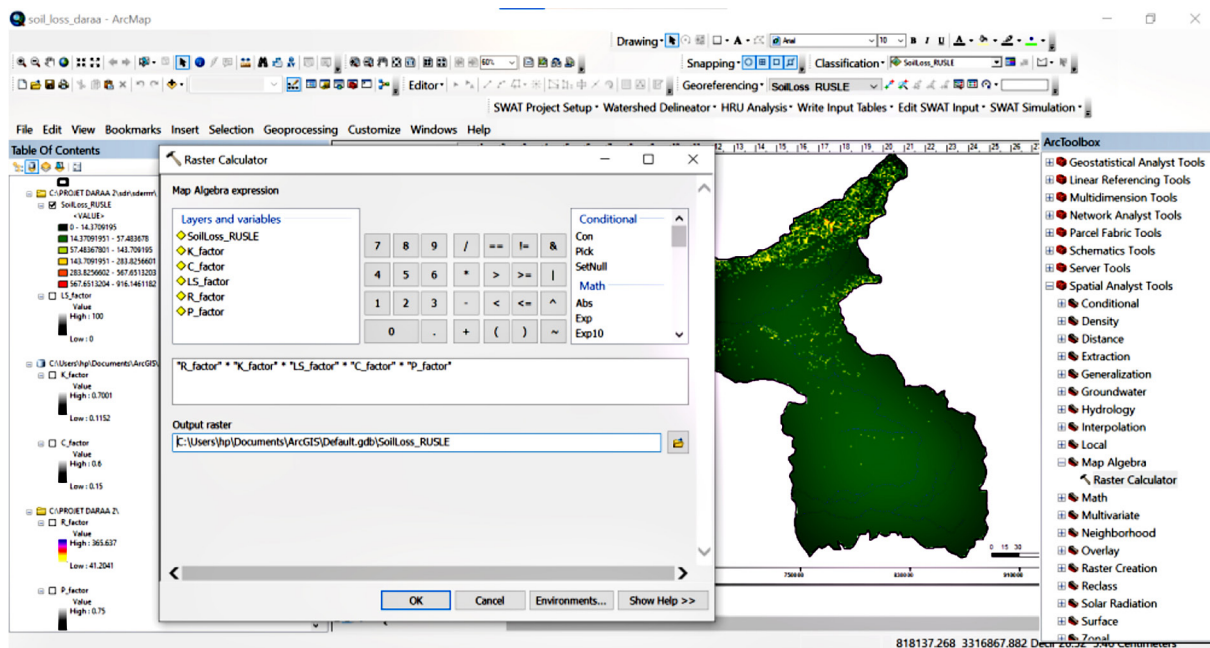


Figure 7. Raster calculator workflow used to compute soil loss based on the RUSLE factors (R, K, LS, C, and P) in the High and Middle Drâa watershed

The synthesis presented in Table 3 confirms this contrast between area extent and erosion contribution: low-severity classes account for most of the surface area, whereas high and extreme erosion classes, despite their restricted spatial extent, represent a major share of estimated soil loss. The ArcGIS 10.1 workflow illustrated in Figure 7, based on the multiplication of R, K, LS, C, and P factors using the Raster Calculator,

further supports this interpretation. Elevated soil loss values observed in the upper parts of the basin therefore primarily reflect morphometric sensitivity (LS), enhanced rainfall aggressiveness (R), and local land-cover and conservation conditions (C and P).

Consequently, classifying soil erosion risk into six categories provides a robust framework for identifying priority areas for soil and water

Table 4. Spatial distribution of sediment delivery ratio (SDR) classes in the High and Middle Drâa watershed

SDR value	Average	Area (ha)	Area (%)
0.000–0.324	0.29	1 346 280	35.43
0.325–0.367	0.35	821 465	21.62
0.368–0.403	0.39	518 972	13.66
0.404–0.440	0.42	409 183	10.77
0.441–0.513	0.48	704 100	18.52
Total	—	3 800 000	100.00

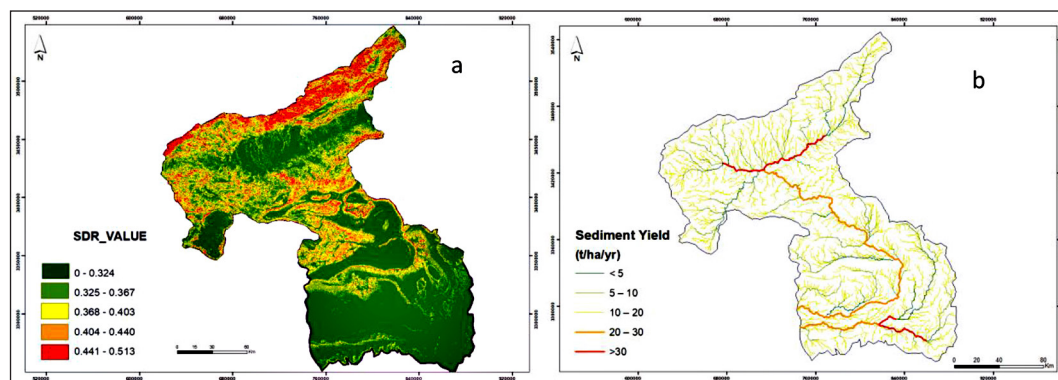


Figure 8. SDR value (a) and sediment yield (b) of the High and Middle Drâa watershed

conservation. Management efforts should focus on upstream erosive hotspots through slope stabilization, vegetation restoration, improved land-use practices, and targeted conservation measures, in order to reduce sediment production and limit downstream impacts within the High and Middle Drâa watershed.

Sediment delivery ratio

The spatial distribution of the sediment delivery ratio (SDR), (Figure 8a) derived from the SDR map and summarized in Table 4, reveals pronounced spatial variability across the High and Middle Drâa watershed. SDR values range from very low to relatively high, reflecting contrasting sediment transfer efficiencies controlled by topography, drainage connectivity, and slope gradients. The lowest SDR class (0.000–0.324) dominates the watershed, covering about 35.43% of the total area. These areas are mainly associated with gently sloping valley bottoms and depositional zones, where sediment transfer capacity is limited and a large proportion of eroded material is retained within the landscape.

Intermediate SDR classes (0.325–0.367 and 0.368–0.403) together account for more than 35% of the watershed area. These zones correspond to moderately connected hillslopes and midstream

sectors, where sediment transport is facilitated but remains partially controlled by internal storage and attenuation processes. In contrast, the highest SDR classes (0.404–0.440 and 0.441–0.513), although spatially restricted and representing less than 30% of the total area, are mainly concentrated in upstream and steeply sloping sectors. These areas exhibit strong channel connectivity and a high capacity to deliver sediments to the drainage network, as confirmed by their elevated average SDR values.

Overall, the results indicate that sediment export from the High and Middle Drâa watershed is controlled by a limited number of highly connected source areas, while large portions of the basin function as sediment sinks. This spatial decoupling between erosion-prone areas and effective sediment delivery highlights the importance of considering landscape connectivity, in addition to soil loss rates, when assessing sediment dynamics and prioritizing soil and water conservation measures.

Sediment yield in the High and Middle Drâa watershed was estimated from the intersection between the soil loss raster and the SDR. The resulting sediment yield values exhibit a wide spatial variability along the drainage network, with classes ranging from less than 5 t·ha⁻¹·yr⁻¹ to values exceeding 30 t·ha⁻¹·yr⁻¹ (Figure 8b). The

Table 5. Channel sediment yield classes and estimated sediment delivery in the High and Middle Drâa watershed

SY ($t \cdot ha^{-1} \cdot yr^{-1}$)	SY class	Area (ha)	Area (%)	SY ($t \cdot yr^{-1}$)
0–5	Low	21 640.35	35.10	39 951
5–10	Moderate	13 280.42	21.55	74 882
10–15	High	8 120.68	13.18	75 243
15–20	Very high	5 210.94	8.45	124 601
> 20	Severe	13 420.61	21.72	771 300
Total	—	61 672.99	100.00	1 085 977

lowest sediment yield class ($<5 t \cdot ha^{-1} \cdot yr^{-1}$) represents the largest proportion of the channel surface, accounting for about 35% of the total drainage area (Table 5). These low-yield segments are mainly associated with gently sloping reaches and low-connectivity sections, where sediment transfer capacity remains limited.

Moderate and high sediment yield classes (5–10 and 10–15 $t \cdot ha^{-1} \cdot yr^{-1}$) together cover more than one third of the channel surface, reflecting intermediate transport conditions along midstream reaches. In contrast, very high and severe sediment yield classes (15–20 and $>20 t \cdot ha^{-1} \cdot yr^{-1}$), although spatially restricted, are concentrated along the main channel and steep upstream tributaries. These sections exhibit a high sediment delivery efficiency and contribute disproportionately to the total sediment load, with an estimated contribution exceeding 70% of the overall channel sediment yield (Table 5).

Overall, the spatial pattern of sediment yield closely mirrors that of the SDR distribution, confirming the dominant role of drainage connectivity and channel slope in controlling sediment export. Despite the high potential soil loss estimated at the watershed scale, only a limited fraction of mobilized sediment is effectively transported through the channel network toward the outlet. A substantial proportion of sediments therefore remains trapped within channels and adjacent depositional zones, highlighting the buffering capacity of the High and Middle Drâa watershed and the importance of channel-scale processes in regulating sediment transfer.

DISCUSSION

The spatial patterns of soil erosion in the High and Middle Drâa watershed highlight the dominant role of topographic and surface characteristics in controlling erosion processes in semi-arid

Moroccan environments. As shown in the soil loss map (Figure 6) and summarized in Table 3, very slight to slight erosion classes (0–14 and 14–57 $t \cdot ha^{-1} \cdot yr^{-1}$) cover more than 61% of the watershed area. However, these classes contribute less than 4% of the total estimated soil loss, indicating that large low-relief sectors function mainly as sediment storage and accumulation zones. Similar distributions have been reported in several Moroccan watersheds, where extensive low-erosion areas coexist with localized erosion hotspots (Sadiki et al., 2004; Taher et al., 2022; Tahiri, 2014).

In contrast, high to extreme erosion classes (144–284, 284–568, and 568–916 $t \cdot ha^{-1} \cdot yr^{-1}$) represent only about 28% of the watershed area but account for more than 90% of the total annual soil loss, estimated at approximately 6.36 million tons per year (Table 3). The extreme erosion class alone contributes nearly 47% of total soil loss while occupying just 11.1% of the basin. This strong imbalance between areal extent and erosion contribution confirms that soil erosion in the Drâa watershed is driven by a limited number of highly vulnerable zones, mainly located in the upstream mountainous areas. These zones are characterized by steep slopes, long slope lengths, sparse vegetation cover, and locally high rainfall aggressiveness, conditions known to amplify the LS and C factors in the RUSLE framework (Wischmeier and Smith, 1978; Renard et al., 1997). Comparable findings have been documented in the Rif and Middle Atlas watersheds, where erosion intensity is strongly controlled by slope morphology rather than by basin-wide climatic averages (Yjjou et al., 2014; Khali Issa et al., 2010; El Amarty et al., 2024).

The SDR analysis further refines the interpretation of erosion dynamics by accounting for sediment transfer efficiency within the drainage network. As illustrated in Figure 8a and reported in Table 4, low SDR values (0.000–0.324) dominate the watershed, covering approximately

35.43% of the total area. These low-connectivity zones correspond mainly to valley bottoms and low-gradient sectors, where sediment transport capacity is limited and a large proportion of eroded material is retained within the landscape. Similar low average SDR values have been reported for large semi-arid Moroccan basins, indicating the importance of internal sediment storage processes (Briak et al., 2016; Taher et al., 2022).

Intermediate SDR classes (0.325–0.403) represent more than 35% of the watershed and are associated with moderately connected hillslopes and midstream areas, where sediment transfer is partial and strongly conditioned by local topography and channel organization. In contrast, the highest SDR classes (0.404–0.513), although spatially restricted and covering less than 30% of the basin area, are concentrated in steep upstream sectors and along well-incised channel segments. These areas exhibit strong hydrological connectivity and enhanced sediment delivery capacity, confirming the positive relationship between slope gradient, drainage density, and sediment transport efficiency reported in previous Moroccan studies (Sadiki et al., 2004; Boufala et al., 2020).

Sediment yield mapping at the channel scale (Figure 8b) clearly reflects this connectivity-driven behavior. According to Table 5, the lowest sediment yield class ($<5 \text{ t}\cdot\text{ha}^{-1}\cdot\text{yr}^{-1}$) represents the largest proportion of the drainage surface (about 35.1%), yet contributes less than 4% of the total channel sediment yield. Conversely, severe sediment yield classes ($>20 \text{ t}\cdot\text{ha}^{-1}\cdot\text{yr}^{-1}$) occupy only 21.7% of the channel area but account for more than 70% of the total sediment delivered through the drainage network, estimated at approximately 1.09 million tons per year. Similar channel-scale contrasts have been observed in the Sebou and Oum Er-Rbia watersheds, where sediment export is controlled by a limited number of highly energetic channel reaches rather than by the entire drainage network (Briak et al., 2016; Taher et al., 2022).

Overall, the results demonstrate that erosion and sediment dynamics in the High and Middle Drâa watershed are governed by a strong spatial decoupling between erosion sources and effective sediment export. While large portions of the basin act as sediment sinks, upstream erosion hotspots and highly connected channel segments play a disproportionate role in sediment production and transfer. These findings are consistent with previous Moroccan studies and confirm the relevance

of combining RUSLE-based soil loss estimation with SDR analysis to identify priority areas for soil and water conservation in data-scarce semi-arid environments (Renard et al., 1997; Sadiki et al., 2004; Yahya and Nawaiseh, 2015).

CONCLUSIONS

The High and Middle Drâa watershed, located in the arid to semi-arid southeastern region of Morocco, represents one of the largest and least studied hydrological systems in the country. Similar to other large Mediterranean and arid watersheds, it is characterized by strong geomorphological contrasts, episodic hydrological activity, and pronounced internal sediment storage. However, unlike many Mediterranean basins that have been extensively investigated, the Drâa system has received limited scientific attention, and existing studies have often addressed it in a fragmented manner by focusing on isolated sub-basins or specific valley sections.

The present study demonstrates that analyzing the High and Middle Drâa watershed as a single integrated system provides a more coherent understanding of erosion and sediment dynamics in large arid basins. The results show that, despite high potential soil erosion in upstream mountainous areas, sediment export at the basin scale remains limited due to strong internal storage and variable landscape connectivity. This confirms that, in large arid and Mediterranean-type watersheds, erosion intensity alone is insufficient to explain sediment yield patterns.

A key scientific contribution of this work lies in the quantitative identification of a spatial and functional decoupling between soil erosion and sediment export across a large, environmentally heterogeneous watershed. By combining the High and Middle Drâa sectors within a unified RUSLE-based and connectivity-oriented framework, the study reveals that sediment transfer is controlled by a restricted number of highly connected slopes and channel segments, while extensive areas of the basin function as long-term sediment sinks. Such behavior is characteristic of large arid Mediterranean basins but has rarely been documented quantitatively for Moroccan watersheds of comparable size and climatic conditions.

By addressing the Drâa watershed as a whole, this study fills an important knowledge gap in erosion and sediment research in arid southern

Morocco. It demonstrates the relevance of using RUSLE not only as a mapping tool, but also as a basis for functional analysis of sediment dynamics in data-scarce environments. The findings open new perspectives for future research on large Moroccan and Mediterranean arid basins, particularly in relation to climate variability, reservoir sedimentation, and basin-scale land management. From a practical standpoint, the results suggest that soil and water conservation strategies should prioritize connectivity hotspots rather than focusing exclusively on areas of maximum soil loss, in order to effectively reduce sediment transfer in arid and semi-arid regions.

REFERENCES

- Amellah, O., El Morabiti, K. (2021). Assessment of soil erosion risk severity using GIS, remote sensing and RUSLE model in Oued Laou Basin (north Morocco). *Soil Science Annual*, 72(3), Article 142530. <https://doi.org/10.37501/soilsa/142530>
- Andualem, T. G., Hewa, G. A., Myers, B. R., Peters, S., Boland, J. (2023). Erosion and sediment transport modeling: A systematic review. *Land*, 12(7), 1396. <https://doi.org/10.3390/land12071396>
- Belasri, A., Lakhouli, A. (2016). Estimation of soil erosion risk using the universal soil loss equation (USLE) and geo-information technology in Oued El Makhazine watershed, Morocco. *Journal of Geographic Information System*, 8(1), 98–107. <https://doi.org/10.4236/jgis.2016.81010>
- Bewket, W., Teferi, E. (2009). Assessment of soil erosion hazard and prioritization for treatment at the watershed level: Case study in the Chemoga watershed, Blue Nile Basin, Ethiopia. *Land Degradation & Development*, 20, 609–622. <https://doi.org/10.1002/ldr.944>
- Boufala, M., El Hmaidi, A., Chadli, K., Essahlaoui, A., El Ouali, A., Lahjouj, A. (2020). Assessment of the risk of soil erosion using RUSLE method and SWAT model at the M'dez watershed, Middle Atlas, Morocco. *E3S Web of Conferences*, 150, 03014. <https://doi.org/10.1051/e3sconf/202015003014>
- Bou-Imajane, L., Belfoul, M. A., Elkadiri, R., Stokes, M. (2020). Soil erosion assessment in a semi-arid environment: A case study from the Argana Corridor, Morocco. *Environmental Earth Sciences*, 79(18), Article 460. <https://doi.org/10.1007/s12665-020-09127-8>
- Boudhar, A., Hanich, L., Boulet, G., Duchemin, B., Berjamy, B., Chehbouni, A. (2009). Evaluation of the Snowmelt Runoff Model in the Moroccan High Atlas Mountains using two snow-cover estimates. *Hydrological Sciences Journal*, 54(6), 1094–1113. <https://doi.org/10.1623/hysj.54.6.1094>
- Briak, H., Moussadek, R., Aboumaria, K., Mrabet, R. (2016). Assessment of sediment yield in a gauged watershed in northern Morocco using SWAT and GIS techniques. *International Soil and Water Conservation Research*, 4(3), 177–185. <https://doi.org/10.1016/j.iswcr.2016.08.002>
- De Jong, S. M. (1994). Applications of reflective remote sensing for land degradation studies in a Mediterranean environment. GéoProdig, portail d'information géographique.
- Desmet, P. J. J., Govers, G. (1996). A GIS procedure for automatically calculating the USLE LS factor on topographically complex landscape units. *Journal of Soil and Water Conservation*, 51(5), 427–433. <https://doi.org/10.1080/00224561.1996.12457102>
- El Amarty, F., Lahrach, A., Benaabidate, L., Chakir, A. (2024). Estimating soil erosion and sediment yield using GIS in the Central Pre-Rif (Northern Morocco): The case of the Oued Lebene watershed. *Ecological Engineering & Environmental Technology*, 25(8), 1–16. <https://doi.org/10.12912/27197050/187977>
- El Jazouli, A., Barakat, A., Ghafiri, A., El Moutaki, S., Ettaqy, A., Khellouk, R. (2017). Soil erosion modeled with USLE, GIS, and remote sensing: A case study of Ikkour watershed in Middle Atlas (Morocco). *Geoscience Letters*, 4, Article 25. <https://doi.org/10.1186/s40562-017-0091-6>
- Gebrehiwot, S. G., Bewket, W., Gärdenäs, A. I., Bishop, K. (2014). Forest cover change over four decades in the Blue Nile Basin, Ethiopia: Comparison of three watersheds. *Regional Environmental Change*, 14(1), 253–266. <https://doi.org/10.1007/s10113-013-0483-x>
- Johannsen, I. M., Hengst, J. C., Goll, A., Höllermann, B., Diekkrüger, B. (2016). Future of water supply and demand in the Middle Drâa Valley, Morocco, under climate and land use change. *Water*, 8(8), 313. <https://doi.org/10.3390/w8080313>
- Khali Issa, L., Raissouni, A., El Arrim, A., Moussadek, R. (2014). Mapping and assessment of water erosion in the Khmiss watershed (northwestern Rif, Morocco). *Journal of Current Advances in Environmental Sciences*, 2, 119–130.
- Maidment, D. R. (1993). *Handbook of hydrology*. McGraw-Hill.
- Mattingly, D., Bokbot, Y., Sterry, M., Cuénod, A., Fenwick, C., Gatto, M. C., Ray, N., Rayne, L., Janin, K., Lamb, A., Niccoló, M., Nikolaus, J. (2018). Long-term history in a Moroccan oasis zone: The Middle Draa Project. *Journal of African Archaeology*, 15(2), 141–172. <https://doi.org/10.1163/21915784-12340009>
- Meliho, M., Boulmane, M., Khattabi, A., Dansou, C. E., Orlando, C. A., Mhammdi, N., Noumonvi, K. D. (2023). Spatial prediction of soil organic carbon

- stock in the Moroccan High Atlas using machine learning. *Remote Sensing*, 15(10), 2494. <https://doi.org/10.3390/rs15102494>
19. Mitasova, H., Hofierka, J., Zlocha, M., Iverson, L. R. (1996). Modelling topographic potential for erosion and deposition using GIS. *International Journal of Geographical Information Systems*, 10(5), 629–641. <https://doi.org/10.1080/02693799608902101>
 20. Moore, I. D., Burch, G. J. (1986). Physical basis of the length-slope factor in the Universal Soil Loss Equation. *Soil Science Society of America Journal*, 50(5), 1294–1298. <https://doi.org/10.2136/sssaj1986.03615995005000050042x>
 21. Morgan, R. P. C. (2005). *Soil erosion and conservation (3rd ed.)*. Blackwell Publishing.
 22. Panagos, P., Borrelli, P., Poesen, J., Ballabio, C., Lugato, E., Meusburger, K., Montanarella, L., Alewell, C. (2015). The new assessment of soil loss by water erosion in Europe. *Environmental Science & Policy*, 54, 438–447. <https://doi.org/10.1016/j.envsci.2015.08.012>
 23. Renard, K. G., Foster, G. R., Weesies, G. A., McCool, D. K., Yoder, D. C. (1997). *Predicting soil erosion by water: A guide to conservation planning with the Revised Universal Soil Loss Equation (RUSLE) (Agriculture Handbook No. 703)*. U.S. Department of Agriculture, Agricultural Research Service.
 24. Sadiki, A., Bouhlassa, S., Auajjar, J., Faleh, A., Maicaire, J. J. (2004). Use of GIS for the evaluation and mapping of erosion risk by the Universal Soil Loss Equation in the Eastern Rif (Morocco): Boussouab watershed case study. *Scientific Institute Bulletin, Earth Sciences Series*, 26, 69–79.
 25. Taher, M., Mourabit, T., Bourjila, A., Saadi, O., Er-rahmouni, A., El Marzkioui, F., El Mousaoui, M. (2022). An estimation of soil erosion rate hot spots by integrated USLE and GIS methods: A case study of the Ghiss dam and basin in northeastern Morocco. *Geomatics and Environmental Engineering*, 16(2), 95–110. <https://doi.org/10.7494/geom.2022.16.2.95>
 26. Tahiri, M. (2014). Évaluation et quantification de l'érosion et de la sédimentation à partir des modèles RUSLE, MUSLE et deposition intégrés dans un SIG: Application au sous-bassin de l'oued Sania (bassin de Tahaddart, Rif nord-occidental, Maroc). *European Journal of Scientific Research*, 125, 57–178.
 27. Van der Knijff, J. M., Jones, R. J. A., Montanarella, L. (2000). *Soil erosion risk assessment in Europe*. European Commission, Joint Research Centre, Space Applications Institute. https://esdac.jrc.ec.europa.eu/content/soil-erosion-risk-assessment-europe?utm_source
 28. Werner, A., Gallagher, M., Weeks, S. (2006). Regional-scale, fully coupled modelling of stream–aquifer interaction in a tropical catchment. *Journal of Hydrology*, 328(3–4), 497–510. <https://doi.org/10.1016/j.jhydrol.2005.12.034>
 29. Williams, J., Nearing, M., Nicks, A., Skidmore, E., Valentin, C., King, K., Savabi, R. (1996). Using soil erosion models for global change studies. *Journal of Soil and Water Conservation*, 51(5), 381–385.
 30. Wischmeier, W. H., Smith, D. D. (1978). *Predicting rainfall erosion losses: A guide to conservation planning (USDA Agriculture Handbook No. 537)*. U.S. Department of Agriculture.
 31. Yahya, F., Nawaiseh, S. (2015). Spatial assessment of soil erosion risk using RUSLE and GIS techniques. *Environmental Earth Sciences*, 74(6), 4649–4669. <https://doi.org/10.1007/s12665-015-4430-7>
 32. Yjjou, M., Bouabid, R., El Hmaidi, A., Essahlaoui, A., El Abassi, M. (2014). Modélisation de l'érosion hydrique via les SIG et l'équation universelle des pertes en sol au niveau du bassin versant de l'Oum Er-Rbia. *The International Journal of Engineering and Science*, 3, 83–91.
 33. Zema, D. A., Bombino, G., Denisi, P., Lucas-Borja, M. E., Zimbone, S. M. (2018). *Evaluating the effects of check dams on channel geometry, bed sediment size and riparian vegetation in Mediterranean mountain torrents*. *Science of the Total Environment*, 642, 327–340. <https://doi.org/10.1016/j.scitotenv.2018.06.035>